Observability of a heavy Higgs boson at hadron supercolliders

U. Baur
Physics Department, University of Wisconsin, Madison, Wisconsin 53706

E. W. N. Glover
Fermi National Accelerator Laboratory, P.O. Box 500, Batavia, Illinois 60510
(Received 21 August 1990)

We present a coherent analysis of Higgs-boson production in the channels $pp \to ZZX \to l^+l^-l'^+l'^-X$ $(l,l'=e,\mu)$ and $pp \to ZZX \to l^+l^-\nu\bar{\nu}X$ $(\nu=\nu_e,\nu_\mu,\nu_\tau)$ for $m_H \geq 600$ GeV at hadron supercolliders, using the exact matrix elements for $gg \to ZZ$ and $qq \to qqZZ$. The importance of a complete understanding of the shape of the perturbative $pp \to ZZX$ background from nonresonant diagrams is emphasized. We find that for the CERN Large Hadron Collider (LHC) to have a Higgs-boson discovery potential comparable to that of the Superconducting Super Collider (SSC) requires at least a factor of 10 times more integrated luminosity. In particular, assuming an integrated luminosity of 10^4 pb^{-1} and perfect lepton identification efficiency, the LHC (SSC) can identify Higgs bosons as resonances with mass up to 600 (800) GeV in $pp \to ZZX \to l^+l^-l'^+l'^-X$. To extend the discovery range of the LHC to $m_H = 800$ GeV in this channel requires an integrated luminosity of at least 10^5 pb^{-1}. For $m_H > 800$ GeV, a clear resonance structure is missing; however, one can still discriminate between a heavy Higgs boson with $m_H \sim 1$ TeV and a light Higgs boson ($m_H \lesssim 2M_z$) at the SSC.

I. INTRODUCTION

One of the main goals of present and future accelerators is the search for the Higgs boson. Its discovery would constitute a significant confirmation of the standard model (SM) of electroweak interactions. Current data from experiments at the CERN Large Electron Positron Collider (LEP) [1] place a lower limit on the Higgs-boson mass of $m_H \gtrsim 44$ GeV. Ultimately, LEP I experiments will be sensitive to Higgs-boson masses up to ~ 50 GeV [2], while at LEP II, one can search for a Higgs boson with mass up to at least 80 GeV in the reaction $e^+e^- \to ZH$ [3].

For larger values of m_H, it is proposed to search for the Higgs boson at hadron supercolliders such as the CERN Large Hadron Collider (LHC) (pp collisions at $\sqrt{s}=16$ TeV) or the Superconducting Super Collider (SSC) (pp collisions at $\sqrt{s}=40$ TeV). Beneath the Z-boson-pair threshold $m_H < 2M_Z$, the analysis is complicated by large QCD backgrounds which overwhelm the signal from the dominant $H \to b\bar{b}$ decay. On the other hand, provided $m_H > 2M_Z$, the decay modes $H \to ZZ \to l^+l^-l'^+l'^-$ $(l,l'=e,\mu)$ and $H \to ZZ \to l^+l^-\nu\bar{\nu}$ $(\nu=\nu_e,\nu_\mu,\nu_\tau)$ both offer good opportunities to discover the Higgs boson. Decays into four charged leptons lead to a very clean signature, while $H \to ZZ \to l^+l^-\nu\bar{\nu}$ results in a rather large number of events because of the large $Z \to \nu\bar{\nu}$ branching ratio [4].

The dominant production mechanism for Higgs bosons in the ZZ channel at hadron colliders are gluon fusion [5–7],

$$gg \to H \to ZZ \ , \tag{1.1}$$

where the gluons couple through a top-quark loop to the Higgs boson, and vector-boson fusion [8–10],

$$qq \to qqH \to qqZZ \ , \tag{1.2}$$

where the initial quarks or antiquarks each radiate a W or Z boson, which then annihilate into a Higgs boson. The cross section of the gluon-fusion process (1.1) depends strongly on the unknown top-quark mass m_t. Present data [11] require $m_t > 89$ GeV, which indicates that the gluon-fusion process dominates at the SSC provided $m_H \lesssim 600$ GeV. On the other hand, the vector-boson fusion process (1.2) contributes substantially to the total Higgs-boson production cross section for larger Higgs-boson masses.

Analytic expressions for $gg \to ZZ$ and $qq \to qqZZ$ matrix elements, which include all contributions from nonresonant Feynman diagrams, have recently been presented in Refs. [7] and [12]. In this paper we use these matrix elements to make a coherent analysis of Higgs-boson production in the $pp \to ZZX \to l^+l^-l'^+l'^-X$ and $pp \to ZZX \to l^+l^-\nu\bar{\nu}X$ channels at hadron supercolliders. In Sec. II we present results for the Z-boson-pair invariant-mass distribution and the ZZ transverse-mass spectrum by combining the cross sections from $q\bar{q} \to ZZ$, $gg \to ZZ$, and $qq \to qqZZ$. We show that a full understanding of the shape of the perturbative $pp \to ZZX$ background from nonresonant diagrams is crucial in order to successfully search for a heavy Higgs boson (or any other strongly interacting scalar sector) at the LHC and SSC. We also demonstrate that the hadron calorimeter of a LHC (SSC) experiment must cover at least the rapidity range of $|\eta| < 4$ (4.5) so that the $H \to ZZ \to l^+l^-\nu\bar{\nu}$ signal is not completely overwhelmed by the $Z+n$ jet, $n \geq 1$, "fake" background. This fake background arises when jets accompanying a Z boson have rapidities outside the range covered by the calorimeter and thus contribute to the missing transverse momentum of the event.

In Sec. III we use the results of the previous section to study in detail the observability of a Higgs boson with mass $m_H \geq 600$ GeV at both the LHC and SSC. We find that, for an integrated luminosity of 10^4 pb^{-1}, the Higgs boson can be identified in the $H \to ZZ \to l^+l^-l'^+l'^-$ channel at the LHC for $m_H \lesssim 600$ GeV. The discovery potential of the LHC can be extended to $m_H \lesssim 800$ GeV by either increasing statistics by a factor of 10 or by searching in the $H \to ZZ \to l^+l^-\nu\bar{\nu}$ channel. Because of the higher center-of-mass energy, the SSC will be able to observe 800 GeV Higgs bosons with an integrated luminosity of only 10^4 pb^{-1}. If the Higgs boson is heavier than about 800 GeV, a clear resonance structure no longer exists. In this case the larger energy available at the SSC may still allow one to clearly separate a strongly interacting Higgs sector from a weakly interacting sector with $m_H < 2M_Z$, while this will be more difficult at the LHC, even with an integrated luminosity of 10^5 pb^{-1}. Finally, we present our conclusions in Sec. IV.

II. CROSS SECTIONS

To compute the cross section for the inclusive reaction $pp \to ZZX$, we use a parton-level Monte Carlo simulation incorporating the lowest-order matrix elements for $q\bar{q} \to ZZ$ [13], $gg \to ZZ$ [7], and $qq \to qqZZ$ [12]. LHC and SSC experiments are expected to cover an electron and muon rapidity range of $|y_l| < 3$. Since about 80% of the charged leptons originating from Z-boson decays have rapidities in the range $|y_Z - y_l| < 0.5$, we approximately simulate the finite lepton coverage of future hadron supercollider experiments, with a rapidity cut on Z bosons decaying into a charged-lepton pair of

$$|y_Z| < 2.5 \ . \tag{2.1}$$

For the two jets in $qq \to qqZZ$, we require a separation in the rapidity-azimuthal-angle plane of

$$\Delta R_{jj} = [(\Delta\phi)^2_{jj} + (\Delta\eta)^2_{jj}]^{1/2} > 0.7 \ . \tag{2.2}$$

This cut is necessary to achieve a finite cross section because of the collinear singularity introduced by photon bremstrahlung diagrams which are incorporated in our calculation and has only a small effect on the total $qq \to qqZZ$ cross section [12].

If both Z bosons decay into charged leptons, the invariant mass m_{ZZ} of the Z pair can be reconstructed and the most obvious strategy to search for the Higgs boson is to look for a resonance structure in the m_{ZZ} spectrum. For large Higgs-boson masses, however, the Higgs width Γ_H, which grows like m_H^3/M_W^2, becomes very large and the resonance peak is significantly diluted. In this case the signal-to-background ratio can be improved by imposing a cut [7,14],

$$p_{TZ} > \tfrac{1}{4} m_{ZZ} \ , \tag{2.3}$$

on the transverse momentum p_{TZ} of the Z bosons. Since the Higgs boson decays isotropically in its center-of-mass frame, one expects to observe a Jacobian peak at $p_{TZ} \approx \frac{1}{2}(m_H^2 - 4M_Z^2)^{1/2}$. The background, on the other hand, is peaked at a low transverse momentum.

Figure 1 shows the ZZ invariant-mass spectrum $B\, d\sigma/dm_{ZZ}$ for $pp \to ZZX \to l^+l^-l'^+l'^-X$ and various Higgs-boson masses at the LHC and SSC. The factor $B = 4.4 \times 10^{-3}$ represents the branching ratio for both Z bosons to decay into electrons or muons. One observes that the Higgs resonance structure is considerably more pronounced at the SSC than at the LHC. This is mostly due to the $q\bar{q} \to ZZ$ background, which is relatively more important at the LHC than at the SSC. Furthermore, the m_{ZZ} spectrum falls somewhat faster at the LHC, being typically a factor 4 smaller at threshold and 10 times smaller at $m_{ZZ} \sim 1$ TeV compared to at the SSC.

While a reasonably clear resonance peak emerges for $m_H \leq 800$ GeV, this is no longer the case for a Higgs boson with mass of the order of 1 TeV. In this case the large width of the Higgs boson ($\Gamma_H \approx 500$ GeV) dilutes the peak and spreads the signal over a large m_{ZZ} range. As a result, the signal of such a "very heavy" Higgs boson constitutes of a rather flat enhancement of the m_{ZZ}

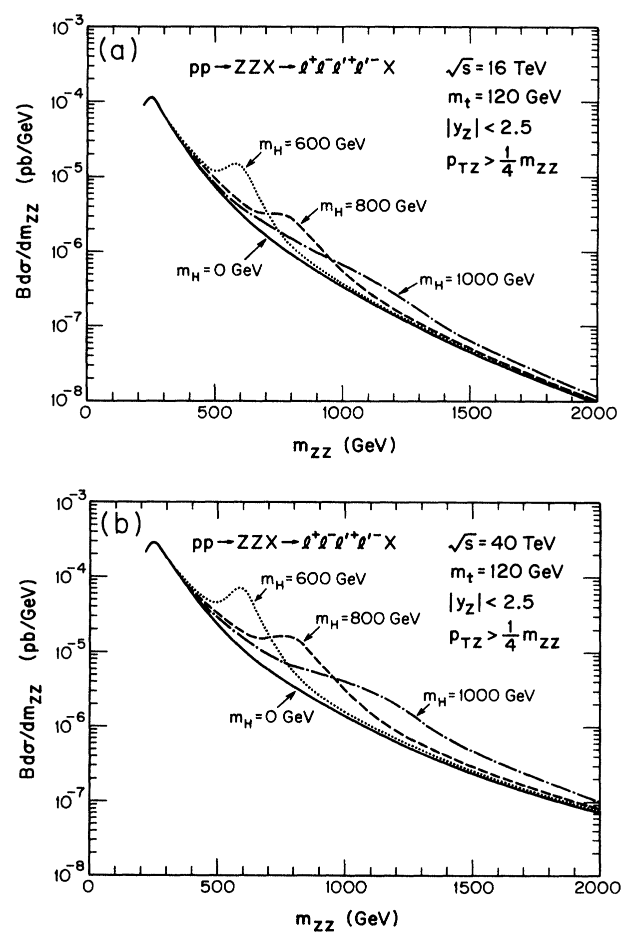

FIG. 1. Invariant-mass distribution $B\, d\sigma/dm_{ZZ}$ of the Z-boson pair in $pp \to ZZX \to l^+l^-l'^+l'^-X$ at (a) the LHC and (b) the SSC, for $m_H = 600$ GeV (dotted line), $m_H = 800$ GeV (dashed line), and $m_H = 1000$ GeV (dot-dashed line). The $m_H = 0$ GeV curve (solid line) represents the perturbative nonresonant background. Both Z bosons are required to have rapidity $|y_Z| < 2.5$ and transverse momentum $p_{TZ} > \frac{1}{4} m_{ZZ}$.

distribution over the perturbative nonresonant background, represented by the solid line labeled $m_H=0$ GeV in Fig. 1. The perturbative nonresonant background is obtained by evaluating the $gg\to ZZ$ and $qq\to qqZZ$ matrix elements with $m_H\sim 0$. In this case the unitarity-violating contributions between Higgs and non-Higgs graphs completely cancel and the resulting m_{ZZ} distribution respects unitarity. In practice, the precise value of m_H is unimportant provided $m_H<2M_Z$.

The SM parameters used in Fig. 1 and all subsequent figures are $m_t=120$ GeV, $\alpha=\alpha(M_Z)=\frac{1}{128}$, $M_Z=91.1$ GeV, $\sin^2\theta_W=0.23$, and $M_W=M_Z\cos\theta_W=80$ GeV. These values are consistent with recent measurements at the SLAC Linear Collider (SLC) [15], LEP [16], and the Fermilab Tevatron [17]. Since in all cases we are probing the hadron structure functions at relatively large x ($\geq 5\times 10^{-3}$), there is little dependence on the choice of input parton distributions. We use the parametrization of Duke and Owens, set I [18] evaluated at momentum scale $Q^2=\hat{s}/4$, where $\hat{s}$ is the parton center-of-mass energy squared. The $O(\alpha_s^2)$ gluon-fusion process is, in principle, sensitive to the choice of scale of the strong coupling constant; however, all scales $\hat{s}$, $p_{TZ}^2+M_Z^2$, m_H^2 etc., are relatively large and different scale choices lead to changes of only $\sim 20\%$; we choose $Q^2=\hat{s}/4$.

The cross section of the gluon-fusion process in the resonance region $m_H-\Gamma_H<m_{ZZ}<m_H+\Gamma_H$ depends significantly on the top-quark mass. For $m_t=120$ GeV, $gg\to ZZ$ is the most important source of 600 GeV Higgs bosons. With increasing m_H, the $qq\to qqZZ$ subprocess gains in importance and becomes competitive with gluon fusion at $m_H\approx 1$ TeV. In the range of m_H we are considering, $m_H\geq 600$ GeV, the $gg\to ZZ$ cross section grows with m_t in the resonance region. For top-quark masses less than 120 GeV, the contribution from gluon fusion is reduced, leading to a slightly less pronounced resonance structure in $d\sigma/dm_{ZZ}$, particularly for smaller Higgs-boson masses. On the other hand, if m_t is significantly larger than 120 GeV, $gg\to ZZ$ would dominate Higgs-boson production for all masses m_H up to ~ 1 TeV, resulting in a considerable enhancement of the Higgs-boson peak in the m_{ZZ} distribution.

In Fig. 2 we show the total cross section $B\sigma(m_{ZZ}>m_{\min})$ above a minimum invariant mass $m_{\min}$ for $pp\to ZZX\to l^+l^-l'^+l'^-X$ at the LHC and SSC as a function of $m_{\min}$. On the right vertical scale, the expected number of events for an integrated luminosity of 10^4 pb^{-1} is indicated. A narrow Higgs boson resonance is characterized in $B\sigma(m_{ZZ}>m_{\min})$ by a sharp drop in the cross section at $m_{\min}=m_H$. This is clearly demonstrated by the dotted line, which shows $B\sigma(m_{ZZ}>m_{\min})$ for $m_H=600$ GeV. For larger Higgs-boson masses, the effect is somewhat washed out by the rapidly increasing width of the Higgs boson; however, the total cross section above a minimum invariant mass is still a rather sensitive indicator of the presence of a Higgs boson. The total cross section for $m_{\min}\geq 1$ TeV is seen to be particularly sensitive to Higgs-boson masses above 800 GeV, where the Higgs boson is strongly coupled [19]. Experimentally, $B\sigma(m_{ZZ}>m_{\min})$ has the advantage of representing data in an unbinned form which can conveniently be analyzed, e.g., by performing a Kolmogorov-Smirnov test. Furthermore, by calculating the difference of the total cross section for two values of $m_{\min}$, one can easily obtain the $pp\to ZZX\to l^+l^-l'^+l'^-X$ cross section for any arbitrary m_{ZZ} mass range.

A heavy Higgs boson with mass $m_H>800$ GeV does not lead to a pronounced resonance structure in $d\sigma/dm_{ZZ}$. Furthermore, the expected event rates at large values of the Z-pair invariant mass are very small. Theoretical predictions for the perturbative nonresonant background must therefore be as accurate as possible if one wants to discriminate a heavy Higgs boson from a light one with $m_H<2M_Z$. In Fig. 3 we show the invariant-mass distribution of the perturbative nonresonant $pp\to ZZX\to l^+l^-l'^+l'^-X$ background (solid line) together with the contributions from the various

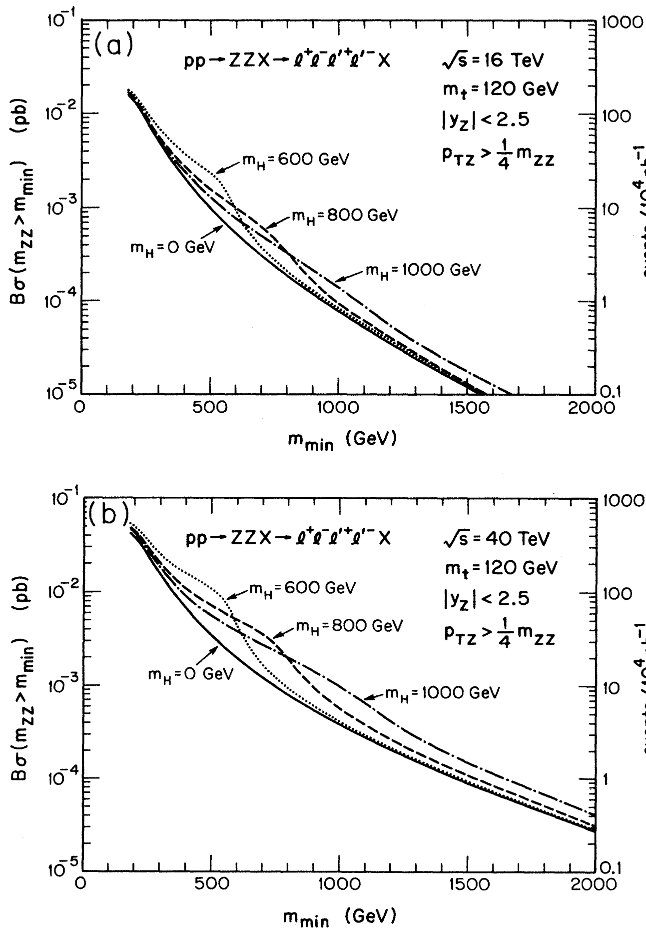

FIG. 2. Total cross section $B\sigma(m_{ZZ}>m_{\min})$ above a minimum invariant mass $m_{\min}$ for $pp\to ZZX\to l^+l^-l'^+l'^-X$ at (a) the LHC and (b) the SSC, for $m_H=600$ GeV (dotted line), $m_H=800$ GeV (dashed line), and $m_H=1000$ GeV (dot-dashed line). The $m_H=0$ GeV curve (solid line) represents the perturbative nonresonant background. Both Z bosons are required to have rapidity $|y_Z|<2.5$ and a transverse momentum $p_{TZ}>\frac{1}{4}m_{ZZ}$.

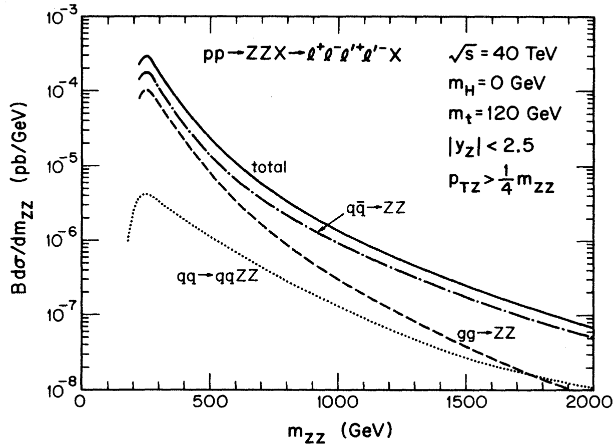

FIG. 3. Invariant-mass distribution of the perturbative nonresonant $pp \to ZZX \to l^+l^-l'^+l'^-X$ background at the SSC. The dotted, dashed, and dot-dashed lines show the contributions from $qq \to qqZZ$, $gg \to ZZ$, and $q\bar{q} \to ZZ$. The solid line gives the sum of the cross sections of the three subprocesses. Both Z bosons are required to have rapidity $|y_Z| < 2.5$ and transverse momentum $p_{TZ} > \frac{1}{4}m_{ZZ}$.

subprocesses at the SSC. One observes that the dominant contribution to the background originates from $q\bar{q} \to ZZ$, with the $gg \to ZZ$ subprocess being the second most important Z-boson-pair source at small values of m_{ZZ}. At large ZZ invariant masses, the $qq \to qqZZ$ subprocess becomes more important than gluon fusion.

Combined, the $gg \to ZZ$ and $qq \to qqZZ$ cross sections represent a 35–60% (14–33%) correction to the $q\bar{q} \to ZZ$ rate at the SSC (LHC). They are thus of the order of magnitude which one expects from the QCD corrections to $q\bar{q} \to ZZ$. These corrections have only been partially computed so far [20] and, therefore, are not included in our calculation. The necessity of an accurate prediction of the perturbative nonresonant $pp \to ZZX$ background, however, clearly warrants a calculation of the complete $O(\alpha_s)$ corrections to $q\bar{q} \to ZZ$.

We now turn to the reaction $pp \to ZZX \to l^+l^-\nu\bar{\nu}X$. Its primary advantage compared to $pp \to ZZX \to l^+l^-l'^+l'^-X$ is the larger branching ratio of $B = 0.026$ for $ZZ \to l^+l^-\nu\bar{\nu}$, which is, approximately, a factor 6 larger than that for $ZZ \to l^+l^-l'^+l'^-$. However, a price has to be paid for the increase in statistics. Since the neutrinos are only detected as missing transverse momentum $\not{p}_T$, the ZZ invariant mass can no longer be reconstructed and one has to consider a transverse-mass variable instead, which leads to a less-pronounced resonance structure. Second, since real detectors do not cover the whole solid angle, potentially dangerous fake backgrounds arise from particles with a rapidity outside the range covered by the detector and which, therefore, generate missing transverse momentum [21].

In our analysis of $pp \to ZZX \to l^+l^-\nu\bar{\nu}X$, we impose a rapidity cut of $|y_Z| < 2.5$ [see Eq. (2.1)] on the Z which decays into the l^+l^- pair, and the jet-jet separation cut (2.2) in the subprocess $qq \to qqZZ$. Furthermore, we require a missing p_T of

$$\not{p}_T > 100 \text{ GeV} . \tag{2.4}$$

This missing-p_T trigger helps to reduce additional fake backgrounds where a nonzero $\not{p}_T$ arises from mismeasurements of momenta, e.g., because of cracks in the detector. Since the Z-pair invariant mass cannot be reconstructed, the p_{TZ} cut (2.3) to enhance the Higgs-boson signal cannot be applied in $pp \to ZZX \to l^+l^-\nu\bar{\nu}X$. The results of our calculations depend in principle on the jet rapidity coverage of the detector, $|\eta_{\rm had}|$, since jets in $qq \to qqZZ$ with rapidity $|\eta| > |\eta_{\rm had}|$ are treated as "missing," and their momentum vector thus contributes to the missing-transverse-momentum vector.

Two different transverse-mass variables are discussed in the literature. The two-body transverse mass of Z pair [22],

$$m_T^2(\mathbf{p}_{TZ},\not{\mathbf{p}}_T) = [(p_{TZ}^2 + M_Z^2)^{1/2} + (\not{p}_T^2 + M_Z^2)^{1/2}]^2 - (\mathbf{p}_{TZ} + \not{\mathbf{p}}_T)^2 , \tag{2.5}$$

depends on the transverse momentum p_{TZ} of the reconstructed Z boson, as well as the missing transverse momentum $\not{p}_T$. On the other hand, the ZZ transverse mass [4]

$$m_{TZZ} = 2(p_{TZ}^2 + M_Z^2)^{1/2} \tag{2.6}$$

only involves the momentum of the Z boson which decays into l^+l^- and is thus easier to handle experimentally. For Z-boson pairs with no transverse momentum, $p_{TZZ} = 0$, $m_T(\mathbf{p}_{TZ},\not{\mathbf{p}}_T)$ and m_{TZZ} coincide. Away from the threshold region, $m_{TZZ} \approx 2p_{TZ}$, and the structure of the Z-boson transverse-momentum spectrum is directly reflected in the m_{TZZ} distribution.

In Fig. 4 we show the m_{TZZ} distribution, $B\, d\sigma/dm_{TZZ}$, at the LHC and SSC for various Higgs-boson masses. For $m_H \leq 800$ GeV, the Higgs boson peak, which is clearly visible in the m_{ZZ} distribution, is degraded to a broad shoulder. The effect of a heavy Higgs boson of mass $m_H \sim 1$ TeV is a smooth, almost structureless, enhancement of the perturbative nonresonant background (solid line), particularly at the LHC. An accurate theoretical prediction of the background will therefore be very important in order to discriminate a heavy Higgs boson from a weakly interacting Higgs in this channel.

The long-dashed lines in Fig. 4 represent the background from $pp \to ZjX \to l^+l^-jX$. This fake background arises when the jet rapidity is outside the range covered by the calorimeter of the detector and thus contributes to the missing transverse momentum of the event [21]. The three long-dashed lines give an estimate of this fake background for a calorimeter coverage of $|\eta_{\rm had}| = 3$, 4, and 4.5 (3.5, 4.5, and 5), respectively, at the LHC (SSC), i.e., when jets with rapidity larger than this value are not identified. Because of the smaller rapidity range covered, the fake $Z\not{p}_TX$ background at the LHC, for a fixed calorimeter coverage $|\eta_{\rm had}|$, is significantly smaller than at the SSC, in particular for large values of $|\eta_{\rm had}|$. Additional, potentially important, contributions to this background arise from $pp \to ZZ + n$ jet with $n \geq 2$. However, these contributions cannot be reliably calculated at present with purely partonic Monte Carlo programs since existing calculations for $Z + n$ jet production [23] ($n \leq 4$) do not take into account soft and virtual corrections. Jet transverse momentum and separation cuts are thus necessary to avoid infrared and collinear singularities and to achieve a finite cross section. If the jets are not observed, these cuts are meaningless and cannot be applied. A calculation which does take into account virtual- and soft-gluon corrections presently only exists for $n=2$ [24]. However, the $pp \to Z + n$ jet contributions will always enhance the $Z\not{p}_T X$ background. The long-dashed lines in

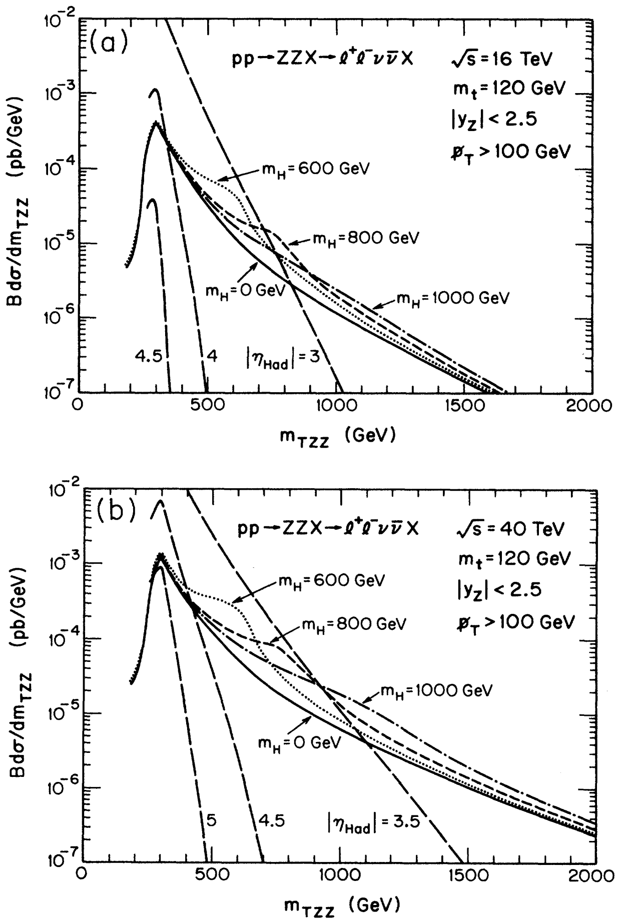

FIG. 4. Z-boson-pair transverse-mass distribution $B\,d\sigma/dm_{TZZ}$ in $pp \to ZZX \to l^+l^-\nu\bar{\nu}X$ at (a) the LHC and (b) the SSC, for $m_H = 600$ GeV (dotted line), $m_H = 800$ GeV (dashed line), and $m_H = 1000$ GeV (dot-dashed line). The $m_H = 0$ GeV curve (solid line) represents the perturbative nonresonant background. The long-dashed curves show the background from $pp \to ZjX \to l^+l^-jX$, where the jet has rapidity $|\eta| > |\eta_{\rm had}|$ and therefore "fakes" missing transverse momentum, for various calorimeter coverages $|\eta_{\rm had}|$. In all cases a $\not{p}_T > 100$ GeV cut and a rapidity cut of $|y_Z| < 2.5$ on the Z decaying into l^+l^- are imposed.

Fig. 4 can thus be viewed as a conservative *lower* bound on the fake $Z\not{p}_T X$ background.

From Fig. 4 it is clear that LHC (SSC) detectors must have a hadron calorimeter covering the rapidity range $|\eta| < 4$ (4.5) if one wants to search for the Higgs boson in $pp \to ZZX \to l^+l^-\nu\bar{\nu}X$. In certain cases, where an accurate determination of the perturbative nonresonant background at low values of m_{TZZ} is important, a coverage out to $|\eta| = 4.5$ (5) may be required. It is important to note that our results are based on a purely parton-level calculation. In practice, hadronic jets are rather more spread than pointlike partonic jets, and an additional coverage rapidity of 0.5 may be necessary to fully contain the jet. Nevertheless, our results for the SSC agree qualitatively with those of Ref. [25].

As we have mentioned above, the m_{TZZ} distribution for $qq \to qqZZ$ depends explicitly on the hadron calorimeter coverage of the detector. The results shown in Fig. 4 (solid, dashed, dotted, and dot-dashed lines) have been obtained assuming that the range out to $|\eta_{\rm had}| = 4$ (4.5) is covered at the LHC (SSC). The dependence of $B\,d\sigma/dm_{TZZ}$ on the calorimeter coverage, however, is quite weak, and almost identical results are obtained, e.g., for $|\eta_{\rm had}| = 2.5$. This is because the two quark jets in $qq \to qqZZ$ typically have a transverse momentum of $\sim 50-100$ GeV, which is much smaller than the missing p_T originating from $Z \to \nu\bar{\nu}$.

One might wonder whether the $pp \to ZjX$ fake background can be reduced by imposing more stringent cuts. It turns out that this is not the case. For example, a rapidity cut of $|y_Z| < 2$ instead (2.1) reduces both signal and background by approximately 20%, without changing the slope of the curves. Alternatively, a more stringent $\not{p}_T$ cut merely increases the m_{TZZ} threshold for both signal and background, and leaves the distributions essentially unchanged at large m_{TZZ}.

There is an additional fake background from the production of $b\bar{b}$, $t\bar{t}$, and W^+W^- pairs, followed by decays into leptons, which can also give rise to a l^+l^- pair accompanied by missing transverse momentum. The size of this background depends on how well lepton pairs from Z decay can be distinguished from continuum production, which, in turn depends on the detector resolution. For the types of detectors under consideration for SSC and LHC experiments, the resolution is sufficiently good that the heavy-quark background is reduced to a level far below the signal [25–27] and does not present a serious problem.

Results very similar to those shown in Fig. 4 are obtained for the $m_T(\mathbf{p}_{TZ}, \not{\mathbf{p}}_T)$ distribution. This can be easily understood by noting that the $q\bar{q} \to ZZ$ and $gg \to ZZ$ subprocesses are the major contributions to the m_{TZZ} and $m_T(\mathbf{p}_{TZ}, \not{\mathbf{p}}_T)$ distributions. In lowest order the Z pair is produced with zero transverse momentum in these two reactions, and in this case, the two distributions coincide. Once higher-order QCD corrections are taken into account, a nonzero p_{TZZ} is generated and the two transverse-mass variables differ on an event-by-event basis. However, in the Higgs resonance region, the ZZ transverse momentum is usually much smaller than the

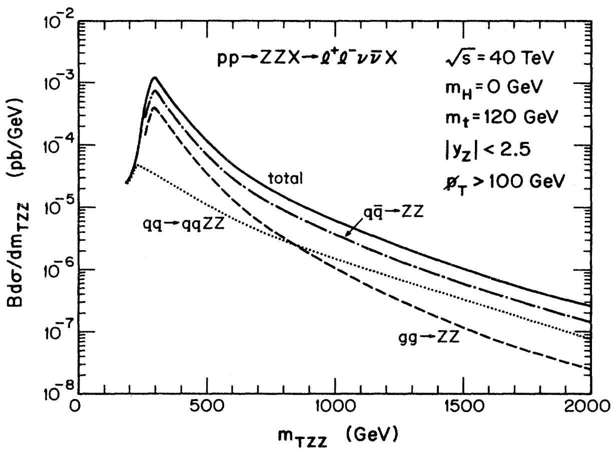

FIG. 5. Z-boson-pair transverse-mass distribution of the perturbative nonresonant $pp \to ZZX \to l^+l^-\nu\bar{\nu}X$ background at the SSC. The dotted, dashed, and dot-dashed lines show the contributions from $qq \to qqZZ$, $gg \to ZZ$, and $q\bar{q} \to ZZ$. The solid line gives the sum of the cross section of the three subprocesses. The Z boson decaying into l^+l^- is required to have rapidity $|y_Z| < 2.5$, and a $\not{p}_t > 100$ GeV cut is imposed.

individual Z-boson p_T, so that the differences between the m_{TZZ} and $m_T(p_{TZ}, \not{p}_T)$ distributions are small in this region. As a further consequence, the transverse momenta of the observed Z boson and the missing p_T tend to balance each other so that the m_{TZZ}, p_{TZ}, and $\not{p}_T$ distributions are all very similar in this region.

One can also study the total cross section above a minimum transverse mass, $B\sigma(m_{TZZ} > m_{T_{\min}})$. The resulting distributions are very similar to those shown in Fig. 2 and thus are not shown.

As we have already emphasized, an accurate prediction of the perturbative nonresonant background will be very important in distinguishing a heavy Higgs boson from a light one. In Fig. 5 we show the m_{TZZ} distribution of the $pp \to ZZX \to l^+l^-\nu\bar{\nu}X$ background (solid line) together with the contributions from the various subprocesses at the SSC. As for the m_{ZZ} distribution (see Fig. 3), the major part of the background originates from $q\bar{q} \to ZZ$ and $gg \to ZZ$. The $qq \to qqZZ$ subprocess is, however, generally more important than it is in $B\,d\sigma/dm_{ZZ}$, particularly at large values of m_{TZZ}. Combined, the $gg \to ZZ$ and $qq \to qqZZ$ cross sections represent a 60–65% ($\sim$30%) correction to the $q\bar{q} \to ZZ$ rate at the SSC (LHC).

III. HIGGS-BOSON DISCOVERY POTENTIAL OF THE LHC AND SSC

To further illustrate the points discussed above, we show in Figs. 6 and 7 the expected number of $pp \to ZZX \to l^+l^-l'^+l'^-X$ and $pp \to ZZX \to l^+l^-\nu\bar{\nu}X$ events versus m_{ZZ} and m_{TZZ}, for various Higgs-boson masses, at the LHC and SSC. The size of the m_{ZZ} and m_{TZZ} bins is 40 GeV. "Data" points show the Higgs-boson signal with statistical errors, while the solid curves represent the perturbative nonresonant background. To transfer cross sections into event rates, we choose two representative luminosities. First, we take $\int \mathcal{L}\,dt = 10^4$ pb^{-1} (lower points and curve), which corresponds to 1 "year" of operation at 10^{33} cm^{-2} s^{-1}. Second, to show the effect of either a higher luminosity of several years of operation, we choose $\int \mathcal{L}\,dt = 10^5$ pb^{-1} (upper points and curve), corresponding to 1 "year" at 10^{34} cm^{-2} s^{-1} or 10 "years" at 10^{33} cm^{-2} s^{-1}. As before, we use $m_t = 120$ GeV and the cuts specified in Eqs. (2.1)–(2.4), and make the additional assumption of a lepton identification efficiency of 100%.

From Fig. 6 it is clear that one should be able to discover a 600 GeV Higgs boson in the $H \to ZZ \to l^+l^-l'^+l'^-$ channel at the LHC with 10^4 pb^{-1} provided $m_t \geq 120$ GeV. However, for a top-quark mass close to its present lower limit, $m_t \approx 90$ GeV [11], the signal of a Higgs boson with $m_H = 600$ GeV only corresponds to a deviation from the perturbative background at the 98% confidence level. (We use a standard χ^2 fit, where, in order to achieve sufficient events in each bin, all events with $m_{ZZ} > 500$ GeV have been collected into a single bin. This procedure guarantees that a high confidence level cannot arise from a single event at high invariant mass.) In this case the value $m_H \sim 600$ GeV seems to mark the Higgs-boson discovery limit for the LHC in $pp \to ZZX \to l^+l^-l'^+l'^-X$ with $\int \mathcal{L}\,dt = 10^4$ pb^{-1}.

It is also evident that an 800 GeV Higgs boson cannot be identified via a resonance structure in the four-charged-lepton mode with only 10^4 pb^{-1} at the LHC and $m_t \leq 120$ GeV, simply because too few events are produced in the resonance region to make the signal observable. If the top-quark mass is significantly larger than 120 GeV, one may, in fact, see a slight enhancement around $m_{ZZ} = 800$ GeV, but even for a 200 GeV top quark, the Higgs resonance peak is not fully visible. On the other hand, provided the fake backgrounds can be controlled, the m_{TZZ} distribution points more directly at the presence of the Higgs boson, and even if $m_t = 90$ GeV, a deviation from the background is observable at the 97% confidence level. Because of the relatively large width of an 800 GeV Higgs boson ($\Gamma_H \approx 260$ GeV), it will not be easy to make a positive identification of such a scalar in the m_{TZZ} distribution. However, with 10^5 pb^{-1}, a clear resonance peak emerges in the four-lepton channel for $m_t \geq 90$ GeV, with at least $\sim$10 events per bin in the resonance region, and an 800 GeV Higgs boson can be discovered at the LHC.

If $m_H > 800$ GeV, the signal is spread out over such a large range that it will be very difficult to see a significant deviation from the perturbative nonresonant background in either channel at the LHC. Even with 10^5 pb^{-1} one can, at best, hope to see a slight systematic increase of the cross section at large invariant masses for $m_t \leq 120$ GeV.

In contrast with the situation at the LHC, an 800 GeV Higgs boson produces a rather clean signal in the m_{ZZ} spectrum at the SSC with 10^4 pb^{-1} (see Fig. 7). Furthermore, because of the much reduced $q\bar{q} \to ZZ$ background, the Higgs signal in the m_{TZZ} spectrum is much more pronounced than at the LHC. Furthermore, the prospects for observing a significant deviation from the perturbative nonresonant background for $m_H > 800$ GeV are much better at the SSC. With an integrated luminosity of 10^5 pb^{-1}, one should be able to clearly discriminate between a heavy Higgs boson with mass $m_H \sim 1$ TeV and a light Higgs boson ($m_H < 2M_Z$) in the four-charged-lepton mode. For 10^4 pb^{-1} this will be considerably more difficult, and the process $pp \to ZZX \to l^+l^-\nu\bar{\nu}X$ with its larger event rate may be helpful.

Figures 6 and 7 clearly demonstrate that in order to observe a statistically significant deviation from the perturbative nonresonant background for $m_H > 800$ GeV, the shape and normalization of the background curve must be known with a high degree of accuracy. This may not be as difficult as it seems for the following reasons. First, although both signal and background are subject to uncertainties in the structure functions and higher order corrections, the relative shapes of signal and background are less uncertain. Second, the normalization will, in practice, be fixed by the data at small m_{ZZ} and m_{TZZ}. (As shown in Fig. 4, some of the small m_{TZZ} data will be contaminated by the fake $Z+n$ jet background, rendering the overall normalization more uncertain.) An accurate measurement of the low mass region will be crucial in extracting any new physics since, in many cases, there is insufficient data at large m_{ZZ} and m_{TZZ} to assist in determining either the shape or normalization.

Our discussion about the observability of a Higgs boson with mass $m_H \geq 600$ GeV has been purely qualitative so far. It can be made somewhat more quantitative be extracting the maximum value $S_{\max} \equiv S(M_{\min}) = \max\{S(m_{\min})\}$ of

$$S(m_{\min}) = \left[\frac{[N_{m_H}(m_{\min}) - N_0(m_{\min})]^2}{N_0(m_{\min})} \right]^{1/2}, \quad (3.1)$$

where $N_{m_H}(m_{\min})$ is the number of signal events for a Higgs boson of mass m_H with $m_{ZZ} > m_{\min}$, and $N_0(m_{\min})$ the corresponding number of background events, in $pp \to ZZX \to l^+l^-l'^+l'^-X$. $N_{m_H}(m_{\min})$ and $N_0(m_{\min})$ are obtained by multiplying $B\sigma(m_{ZZ} > m_{\min})$ (see Fig. 2) with the integrated luminosity. $M_{\min}$ is the value of $m_{\min}$ which maximizes $S(m_{\min})$.

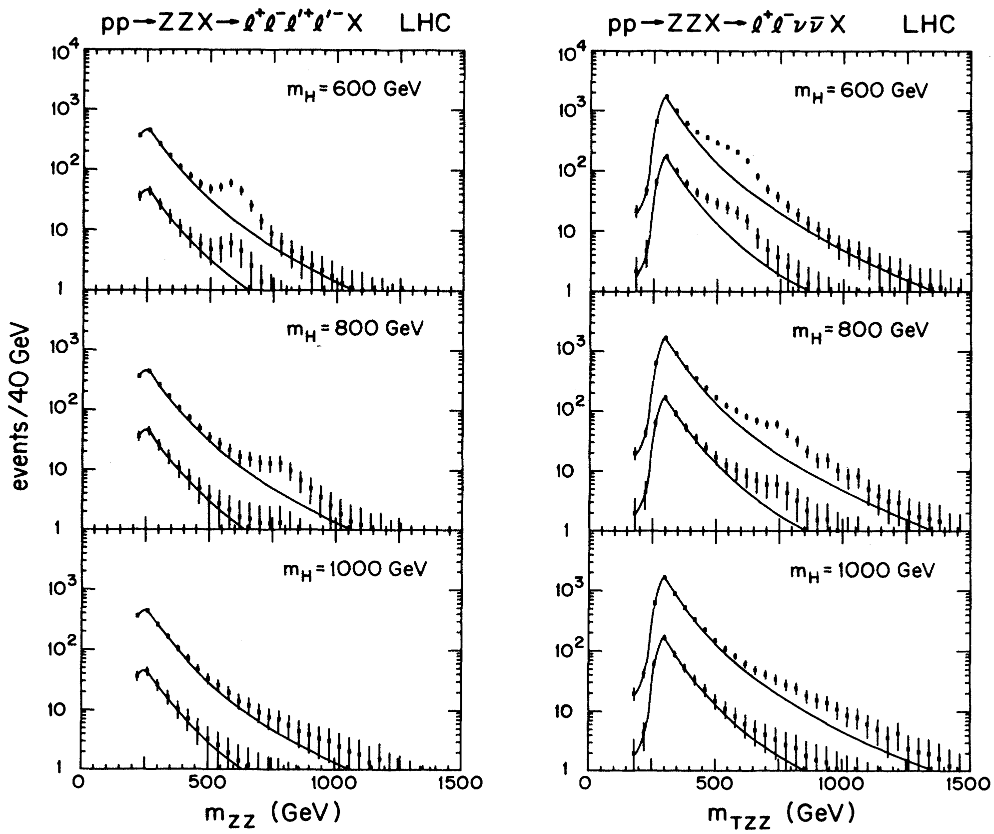

FIG. 6. Expected event rates for $pp \to ZZX \to l^+l^-l'^+l'^-X$ and $pp \to ZZX \to l^+l^-\nu\bar{\nu}X$ as a function of m_{ZZ} and m_{TZZ}, respectively, for $m_H = 600$, 800, and 1000 GeV at the LHC. "Data" points show the Higgs-boson signal in 40-GeV bins with statistical errors, while continuous curves represent the perturbative nonresonant background. Upper (lower) points and curves correspond to an integrated luminosity of 10^5 pb^{-1} (10^4 pb^{-1}). The cuts specified in Eqs. (2.1)–(2.4) are imposed.

S_{max} represents the statistical significance, in standard deviations, of the signal of a Higgs boson with mass m_H. For a narrow resonance, S_{max} is equivalent to the significance of the cross section enhancement in the resonance region. By replacing $N_0(m_{min})$ in Eq. (3.1) by $N_{m'_H}(m_{min})$, $S(m_{min})$ can be generalized so that the corresponding value of S_{max} gives a quantitative measure of how well a Higgs boson with mass m_H can be discriminated from a Higgs boson of mass m'_H at the LHC or SSC. This in turn reflects how well m_H can be measured in $pp \to ZZX \to l^+l^-l'^+l'^-X$. A similar analysis can, in principle, be also carried out for $H \to ZZ \to l^+l^-\nu\bar{\nu}X$. However, because of the $Z+n$ jet fake background, the expected systematic errors in this channel are significantly larger than for the decay into four charged leptons, rendering the results of such an analysis more uncertain, and we have not attempted it.

Table I lists S_{max} and the corresponding value of M_{min} for various Higgs-boson masses m_H and m'_H at the LHC and SSC, for an integrated luminosity of 10^4 pb^{-1} (10^5 pb^{-1}). M_{min}, in general, does not change very much when the center-of-mass energy is increased from 16 to 40 TeV. Furthermore, all values of M_{min} are sufficiently small, so that the number of events is large enough to make this analysis meaningful. From the values of the statistical significance shown in Table I, one can conclude that the *Higgs-boson discovery potential of the LHC with* 10^5 *pb*$^{-1}$ *is roughly equivalent to that of the SSC with* 10^4 *pb*$^{-1}$. *Alternatively, for the LHC to be competitive with the SSC, the LHC must achieve an integrated luminosity at least 10 times larger than that achieved by the SSC.*

At the LHC and with an integrated luminosity of $\int \mathcal{L}\,dt = 10^4$ pb^{-1}, a 600 GeV Higgs boson produces a 4.3σ deviation from the perturbative nonresonant background in the $H \to ZZ \to l^+l^-l'^+l'^-$ channel. On the other hand, using this sort of analysis, it can only be discriminated from a Higgs boson with $m_H = 800$ GeV (1 TeV) at the 2.0σ (2.9σ) level. In this case a direct examination of the invariant-mass distribution should provide a better mass discrimination since the resonance structure of a 600 GeV Higgs boson is clearly visible (see Fig. 6).

In Fig. 6 we have seen that there are too few events to make an 800 GeV Higgs resonance observable at the LHC with $\int \mathcal{L}\,dt = 10^4$ pb^{-1}. Nevertheless, since the signal is spread over a fairly large invariant-mass range,

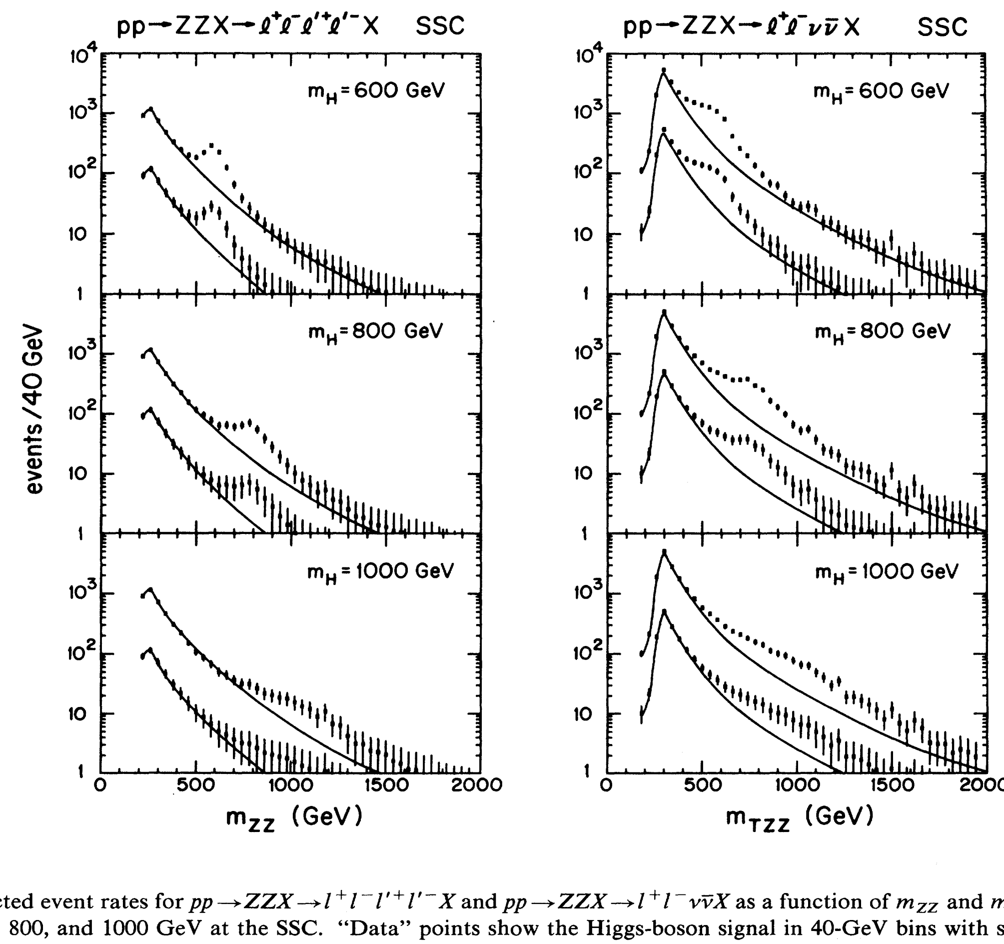

FIG. 7. Expected event rates for $pp \to ZZX \to l^+l^-l'^+l'^-X$ and $pp \to ZZX \to l^+l^-\nu\bar{\nu}X$ as a function of m_{ZZ} and m_{TZZ}, respectively, for $m_H = 600$, 800, and 1000 GeV at the SSC. "Data" points show the Higgs-boson signal in 40-GeV bins with statistical errors, while continuous curves represent the perturbative nonresonant background. Upper (lower) points and curves correspond to an integrated luminosity of 10^5 pb^{-1} (10^4 pb^{-1}). The cuts specified in Eqs. (2.1)–(2.4) are imposed.

TABLE I. Statistical significance of the Higgs-boson signal at the LHC and SSC in $pp \to ZZX \to l^+l^-l'^+l'^-X$, for $m_t = 120$ GeV and an integrated luminosity of 10^4 pb^{-1} (10^5 pb^{-1}). Both Z bosons are required to have rapidity $|y_Z| < 2.5$ and transverse momentum $p_{TZ} > \frac{1}{4} m_{ZZ}$. $S_{\max} \equiv S(M_{\min}) = \max\{S(m_{\min})\}$ represents the significance, in standard deviations, of a Higgs boson with mass m_H compared to the perturbative nonresonant background ($m'_H = 0$) and compared to a Higgs boson with a different mass m'_H. $M_{\min}$ is the value of $m_{\min}$ for which $S(m_{\min})$ [see Eq. (3.1)] is maximal.

		LHC		SSC	
m_H (GeV)	m'_H (GeV)	$M_{\min}$ (GeV)	$S_{\max}$	$M_{\min}$ (GeV)	$S_{\max}$
	0	500	4.3 (13.4)	500	12.7 (40.0)
600	800	460	2.0 (6.5)	420	4.9 (15.5)
	1000	460	2.9 (9.3)	460	7.4 (23.5)
	0	620	2.0 (6.5)	620	7.0 (22.2)
800	600	420	1.7 (5.4)	700	4.4 (13.9)
	1000	580	0.8 (2.5)	580	2.1 (6.7)
	0	700	1.1 (3.5)	700	4.4 (13.9)
1000	600	460	2.2 (7.1)	420	5.4 (17.1)
	800	580	0.7 (2.3)	540	1.9 (5.9)

the total cross section above a minimum invariant mass is significantly larger than the background cross section and leads to a 2.0σ effect for $M_{\min} = 620$ GeV. Although an effect of this size certainly does not establish the existence of a Higgs boson, it demonstrates that $S_{\max}$ is a rather sensitive indicator for such a particle. For $m_t = 200$ GeV, the significance of the Higgs-boson signal is increased to 4.2σ. On the other hand, an 800 GeV Higgs boson clearly produces a strong signal (7.0σ) at the SSC. However, since the width rapidly increases with m_H, it will be more difficult to distinguish it from a heavier Higgs boson than from a lighter scalar (see Table I).

The statistical significance of a 1 TeV Higgs boson at the SSC appears close to that of a 600 GeV Higgs boson at the LHC (both with $\int \mathcal{L}\, dt = 10^4$ pb^{-1}). This apparent equivalence should not be taken too seriously since in one case a clear resonance structure is observable, while in the other, one only observes an almost structureless enhancement over a wide range of m_{ZZ} which is therefore much more susceptible to systematic uncertainties in the shape of the nonresonant background. Nevertheless, Table I clearly shows that for a really heavy Higgs boson with $m_H \sim 1$ TeV, *the SSC offers much better prospects for observing a statistically significant deviation from the perturbative nonresonant background and, thus, for separating a strongly interacting scalar sector from a light, weakly interacting Higgs sector than the LHC.*

The values listed in Table I have been derived by assuming a lepton identification efficiency of 100% and without taking into account any systematic errors. Viewed from this point, they are thus somewhat optimistic. On the other hand, there are more powerful statistical methods available than the one used above to analyze real experimental data, and they may easily lead to a larger significance in cases where there is a localized Higgs resonance structure, and also allow one to discriminate more accurately between different values of m_H. The values of $S_{\max}$ in Table I should therefore be regarded as semiquantitative estimates, illustrating the qualitative statements made above.

IV. SUMMARY AND CONCLUSIONS

In this paper we have presented a coherent analysis of Higgs-boson production in $pp \to ZZX \to l^+l^-l'^+l'^-X$ and $pp \to ZZX \to l^+l^-\nu\bar{\nu}X$ at hadron supercolliders, using the exact matrix elements for $gg \to ZZ$ and $qq \to qqZZ$. We have shown results for the invariant and transverse mass of the Z-boson pair by combining the cross sections from $q\bar{q} \to ZZ$, $gg \to ZZ$, and $qq \to qqZZ$. Furthermore, we have demonstrated that an accurate theoretical prediction of the shape and normalization of the perturbative nonresonant background will be crucial in extracting the Higgs signal, particularly for $m_H > 800$ GeV, where a clear resonance structure no longer exists. Combined, the $gg \to ZZ$ and $qq \to qqZZ$ background cross sections are about the same size as one expects the QCD corrections to $q\bar{q} \to ZZ$ to be. Since the perturbative nonresonant background also constitutes a lower limit on the $pp \to ZZX$ cross section, a calculation of the complete $O(\alpha_s)$ corrections to $q\bar{q} \to ZZ$ is clearly warranted.

In the ZZ transverse-mass distribution m_{TZZ} [see Eq. (2.6)], the Higgs resonance peak is degraded to a broad shoulder. Away from the Z-pair threshold, the m_{TZZ} p_{TZ}, $\not{p}_T$, and the two-body transverse-mass distribution $m_T(\mathbf{p}_{TZ}, \not{\mathbf{p}}_T)$ [see Eq. (2.5)], are all very similar. Furthermore, the dependence of the m_{TZZ} distribution on the rapidity range covered by the calorimeter of the detector is quite weak. However, in order to sufficiently suppress the $pp \to ZjX \to l^+l^-jX$ fake background, LHC (SSC) detectors must have a hadron calorimeter covering the rapidity range $|\eta| < 4$ (4.5) (see Fig. 4).

Based on these results, we have studied the observability of a Higgs boson with mass $m_H \gtrsim 600$ GeV at the LHC and SSC. We find that, for $\int \mathcal{L}\, dt = 10^4$ pb^{-1}, the Higgs boson can be identified at the LHC in the four-charged-lepton decay mode provided $m_H \lesssim 600$ GeV. The range of accessible Higgs-boson masses at the LHC can be extended to $m_H \sim 800$ GeV by either searching in the $H \to ZZ \to l^+l^-\nu\bar{\nu}$ channel or by increasing the integrated luminosity to 10^5 pb^{-1}. In contrast, an 800 GeV Higgs boson produces a very clean signal in $B\, d\sigma/dm_{ZZ}$ at the SSC with only 10^4 pb^{-1}. In other words, for the LHC to fully cover the range $m_H \leq 800$ GeV in the four-charged-lepton mode requires at least 10 times more integrated luminosity than the SSC. If this is not achieved, the Higgs-boson discovery potential of the LHC is not as good as that of the SSC. On the other hand, we find that the LHC with 10^5 pb^{-1} is competitive at identifying heavy Higgs bosons to the SSC with 10^4 pb^{-1}.

For $m_H > 800$ GeV, where the signal, because of the large width of the Higgs boson, consists of a smooth, almost structureless, enhancement of the perturbative nonresonant background (see Figs. 1 and 4), the SSC has a much better chance of observing a statistically significant effect than the LHC. In fact, even if no resonance structure in Z-pair production is observed at the SSC, one should be able to clearly discriminate between a heavy, strongly interacting symmetry-breaking sector and a light perturbative sector characterized by a light Higgs boson with mass $m_H < 2M_Z$, provided that the perturbative nonresonant background is known with sufficient accuracy.

Finally, the conclusions presented here are somewhat more optimistic than those of previous studies, particularly for the LHC [26,27]. The reasons for this are twofold. First and most important, throughout this work, we have assumed a rather large value for the top-quark mass, $m_t = 120$ GeV, some way above the current lower bound, $m_t > 89$ GeV. However, our conclusions are not significantly softened even if the top quark is just around the corner, $m_t \approx 90-95$ GeV. On the other hand, if the top quark is heavier, $m_t \sim 200$ GeV, the Higgs-boson signal will become more pronounced. Second, we utilize the exact matrix elements for Z-boson pair production, which contain some sizable interference effects, especially for $gg \to ZZ$, and which increase the effective size of the signal.

ACKNOWLEDGMENTS

We would like to thank S. Errede, K. Einsweiler, D. Froidevaux, I. Hinchliffe, K. Meier, D. Morris, K. Sliwa, and C. P. Yuan for useful discussions. This research was supported in part by the University of Wisconsin Research Committee with funds granted by the Wisconsin Alumni Research Foundation and in part by the U.S. Department of Energy under Contract No. DE-AC02-76ER00881.

[1] ALEPH Collaboration, D. Decamp *et al.*, Phys. Lett. B **246**, 306 (1990); **245**, 289 (1990); **241**, 141 (1990); **236**, 233 (1990); OPAL Collaboration, M. Z. Akrawy *et al.*, *ibid.* **253**, 511 (1991); Report No. CERN-EP/90-100, 1990 (unpublished); Phys. Lett. B **236**, 224 (1990); DELPHI Collaboration, P. Abreu *et al.*, Nucl. Phys. **B342**, 1 (1990); L3 Collaboration, B. Adeva *et al.*, Phys. Lett. B **252**, 518 (1990); **248**, 203 (1990).

[2] M. Drees *et al.*, in *Z Physics at LEP 1,* Proceedings of the Workshop, Geneva, Switzerland, 1989, edited by G. Altarelli, R. Kleiss, and C. Verzegnazzi (CERN Yellow Report No. 89-08, Geneva, 1989), Vol. 2, p. 58, and references therein.

[3] See, e.g., S. L. Wu *et al.*, in *Proceedings of the ECFA Workshop on LEP 200,* Aachen, Germany, 1986, edited by A. Bohm and W. Hoogland (Report No. CERN 87-08, Geneva, Switzerland, 1987), Vol. II, p. 312, and references therein; Z. Kunszt and W. J. Stirling, Phys. Lett. B **242**, 507 (1990).

[4] R. N. Cahn and M. S. Chanowitz, Phys. Rev. Lett. **56**, 1327 (1986).

[5] H. Georgi, S. L. Glashow, M. E. Machacek, and D. V. Nanopoulos, Phys. Rev. Lett. **40**, 692 (1978).

[6] D. A. Dicus, C. Kao, and W. W. Repko, Phys. Rev. D **36**, 1570 (1987).

[7] E. W. N. Glover and J. J. van der Bij, Phys. Lett. B **219**, 488 (1989); Nucl. Phys. **B321**, 561 (1989).

[8] R. N. Cahn and S. Dawson, Phys. Lett. **136B**, 196 (1984); **138B**, 464(E) (1984); S. Dawson, Nucl. Phys. **B249**, 42 (1984); G. L. Kane, W. W. Repko, and W. B. Rolnick, Phys. Lett. **148B**, 367 (1984).

[9] M. S. Chanowitz and M. K. Gaillard, Phys. Lett. **142B**, 85 (1984).

[10] A. Abbasabadi and W. W. Repko, Nucl. Phys. **B292**, 461 (1987); Phys. Rev. D **37**, 2668 (1988).

[11] CDF Collaboration, F. Abe *et al.*, Phys. Rev. Lett. **64**, 142 (1990); **64**, 147 (1990); K. Sliwa, in *High Energy Hadronic Interactions,* proceedings of the XXVth Rencontre de Moriond, Les Arcs, France, 1990, edited by J. Tran Thanh Van (Editions Frontieres, Gif-sur-Yvette, 1990).

[12] U. Baur and E. W. N. Glover, Nucl. Phys. **B347**, 12 (1990).

[13] R. W. Brown and K. O. Mikaelian, Phys. Rev. D **19**, 922 (1979).

[14] V. Barger, T. Han, and R. J. N. Phillips, Phys. Lett. B **206**, 339 (1988).

[15] Mark II Collaboration, G. S. Abrams *et al.*, Phys. Rev. Lett. **63**, 724 (1989).

[16] L3 Collaboration, B. Adeva *et al.*, Phys. Lett. B **231**, 509 (1989); ALEPH Collaboration, D. Decamp *et al.*, *ibid.* **231**, 519 (1989); OPAL Collaboration, M. Z. Akrawy *et al.*, *ibid.* **231**, 530 (1989); DELPHI Collaboration, P. Aarnio *et al.*, *ibid.* **231**, 539 (1989).

[17] CDF Collaboration, F. Abe *et al.*, Phys. Rev. Lett. **63**, 720 (1989).

[18] D. Duke and J. Owens, Phys. Rev. D **30**, 49 (1984).

[19] M. S. Chanowitz and M. K. Gaillard, Nucl. Phys. **B261**, 379 (1985).

[20] V. Barger, J. L. Lopez, and W. Putikka, Int. J. Mod. Phys. A **3**, 2181 (1988); U. Baur, E. W. N. Glover, and J. J. van der Bij, Nucl. Phys. **B318**, 106 (1989).

[21] R. N. Cahn *et al.*, in *Experiments, Detectors, and Experimental Areas for the Superconducting Super Collider,* proceedings of the Workshop, Berkeley, California, 1987, edited by R. Donaldson and M. G. D. Gilchriese (World Scientific, Singapore, 1987), p. 20.

[22] V. Barger, T. Han, and R. J. N. Phillips, Phys. Rev. D **36**, 295 (1987).

[23] K. Hagiwara and D. Zeppenfeld, Nucl. Phys. **B313**, 560 (1988); F. A. Berends, W. T. Giele, and H. Kuijf, *ibid.* **B321**, 39 (1989); V. Barger, T. Han, J. Ohnemus, and D. Zeppenfeld, Phys. Rev. Lett. **62**, 1971 (1989); Phys. Rev. D **40**, 2888 (1989); F. A. Berends, W. T. Giele, R. Kleiss, H. Kuijf, and W. J. Stirling, Phys. Lett. B **224**, 237 (1989); F. A. Berends, W. T. Giele, H. Kuijf, and B. Tausk, Report No. FERMILAB-PUB-90/213-T 1990 (unpublished).

[24] P. Arnold and M. H. Reno, Nucl. Phys. **B319**, 37 (1989).

[25] R. M. Barnett and I. Hinchliffe, Report No. LBL-28773, SSC-SDE-29, 1990 (unpublished).

[26] D. Froidevaux and B. van Eijk, in Report No. CERN 88-02, 1988, edited by J. H. Mulvey, p. 73.

[27] D. Froidevaux, in *Proceedings of the Workshop on Physics at Future Accelerators,* La Thuile, Italy, 1987, edited by J. H. Mulvey (Report No. CERN 87-07, Geneva, Switzerland, 1987), Vol. 1, p. 61.